Beijing J. of Pure and Appl. Math.
Volume 1, Number 1, 121–158, 2024

Integral iterations for harmonic maps

Andrew Neitzke

Dedicated to Sergio Cecotti, in honor of his profound ideas and generous scientific spirit

We study minimal harmonic maps $g : \mathbb{C} \to \mathrm{SO}(3)\backslash\mathrm{SL}(3,\mathbb{R})$, parameterized by polynomial cubic differentials P in the plane. The asymptotic structure of such a g is determined by a convex polygon $Y(P)$ in $\mathbb{RP}^2$. We give a conjectural method for determining $Y(P)$ by solving a fixed-point problem for a certain integral operator. The technology of spectral networks and BPS state counts is a key input to the formulation of this fixed-point problem. We work out two families of examples in detail.

MSC 2020 subject classifications: Primary 35A25, 58E20; secondary 81Q60.
Keywords and phrases: Harmonic maps, Higgs bundles, spectral networks.

1. Introduction

1.1. Summary

This paper concerns harmonic maps from the flat complex plane to a Riemannian symmetric space,

$$g : \mathbb{C} \to \mathrm{SO}(3)\backslash\mathrm{SL}(3,\mathbb{R}), \tag{1.1}$$

which are *minimal* and have *polynomial growth*. The basic facts about such maps were set out in [2]: as we review in §2.1 below,

- for each degree n polynomial P there is a corresponding minimal harmonic map g, unique up to an $\mathrm{SL}(3,\mathbb{R})$ translation of $\mathrm{SO}(3)\backslash\mathrm{SL}(3,\mathbb{R})$,
- the asymptotic behavior of $g(z)$ as $z \to \infty$ is controlled by a convex $(n+3)$-gon in $\mathbb{RP}^2$, which we call $Y(P)$.

Thus the question arises:

Question 1. *What can we say about the convex $(n+3)$-gon $Y(P)$ corresponding to a given degree n polynomial P?*

The main aim of this paper is to describe a conjectural approach to this question which arises naturally from the work [3, 4, 5].[1] For the most part we do not attempt to explain the motivation, focusing rather on giving enough detail to make it clear precisely what the conjecture is. In short:

Conjecture 1. *When P has only simple zeroes, $Y(P)$ can be computed from the solution of a fixed-point problem for an integral operator acting on collections of functions in one variable ζ, described in §4.1 below.*

The fixed-point problem appearing in Conjecture 1 does not involve the polynomial P directly but rather uses various ingredients derived from P, which are introduced in §3. In particular, it uses the *WKB spectral networks* derived from P, described in §3.3.

In §5 we work out the details of two examples of Conjecture 1: one with $n = 2$ (in §5.1–§5.2), another with $n = 3$ (in §5.3–§5.4).

Conjecture 1 is closely related to an integral iteration introduced much earlier in the context of tt^* geometry [6, 7] and to the thermodynamic Bethe ansatz. It is complementary to the more obvious method of solving the harmonic map equations directly, and exposes different aspects of the underlying structure. Its consequences are especially transparent when we study the asymptotic behavior for large P; this is explained in §4.2–§4.3.

1.2. A sample prediction

Here is a concrete example (from §5.1) of a prediction obtained from Conjecture 1. We consider a 1-parameter family of polynomials:

$$P(z) = \frac{R^3}{2}\left(-z^2+1\right), \qquad R \in \mathbb{R}_+. \tag{1.2}$$

The family (1.2) corresponds to a 1-parameter family of convex pentagons $Y(P)$ in $\mathbb{RP}^2$, up to $\mathrm{SL}(3,\mathbb{R})$ action. Such a pentagon is determined by two invariant cross-ratios, which we denote $(X_{\gamma_1}, X_{\gamma_2})$.[2] The fact that the coefficients in (1.2) are all real leads to a reflection symmetry which implies

[1] More precisely, this paper involves a small extension of [5] to treat connections with a specific sort of irregular singularity.

[2] For the definition of X_{γ_i} in terms of the vertices of the pentagon, see (5.4) below.

$X_{\gamma_2}(R) = 1$ for all R, so only $X_{\gamma_1}(R)$ remains to be determined. We predict (see (5.7) below)

(1.3)
$$X_{\gamma_1}(R) = \exp\left(aR - \frac{3}{2\sqrt{\pi\rho R}}\mathrm{e}^{-2\rho R} + \delta(R)\right), \quad a \approx -4.00648, \quad \rho \approx 2.31315,$$

where the remainder function $\delta(R)$ obeys

$$\lim_{R\to\infty} \delta(R)\sqrt{R}\mathrm{e}^{2\rho R} = 0. \tag{1.4}$$

Two features of (1.3) deserve comment:

- The leading behavior of $\log X_{\gamma_1}(R)$ is *linear* in R. The constant a arises as a period: $aR = 2\,\mathrm{Re}\oint_{\gamma_1} P(z)^{1/3}\mathrm{d}z$, where the contour γ_1 is shown in Figure 6 below.
- The subleading behavior of $\log X_{\gamma_1}(R)$ is *exponentially suppressed* in R, and the coefficient of the exponentially suppressed term is explicitly computed.

These two features are aspects of the general Conjecture 1, which recur more generally. In (4.11) below we give the general form of an asymptotic prediction generalizing (1.3).

1.3. Numerical checks

It is possible to subject Conjecture 1 to direct checks. Indeed, Conjecture 1 leads to a numerical scheme for computing the invariants of $Y(P)$, by iteration of the relevant integral operator. On the other hand, one can compute the invariants of $Y(P)$ directly, by solving the harmonic map equations numerically; tools for doing so have been developed by David Dumas and Michael Wolf [1].

In the paper [8], Dumas and I apply both of these methods to the examples in §5, and compare the results; we find that Conjecture 1 indeed holds, to the precision we are able to attain. The possibility of making such a comparison was the main motivation for writing this paper. Moreover, preliminary such comparisons were important in shaking out various mistakes which I made in initial attempts to write §5.

1.4. Contours and clusters

In the example of §1.2 above, the asymptotics of the cross-ratio X_{γ_1} are controlled by a specific period integral over a contour γ_1. This is another feature of the general Conjecture 1: there is a lattice Γ of allowed contours, and for each $\gamma \in \Gamma$, there is a corresponding cross-ratio[3] X_γ, such that the leading asymptotics of X_γ are controlled by the period $\oint_\gamma P(z)^{1/3}\mathrm{d}z$. Moreover, knowing all the cross-ratios X_γ is sufficient to determine the polygon $Y(P)$.

One of the essential points in making Conjecture 1 precise is thus to identify which cross-ratio X_γ corresponds to a given contour γ. This turns out to be rather subtle: to do it, we need the spectral network associated to the polynomial P. Given the network we face the problem of drawing certain compatible *abelianization trees* which determine the X_γ. We have solved this problem by hand for the examples we treat in this paper, but it would be very desirable to have a more general method, or at least to show that a solution always exists. This part of the story is described in §3.3–§3.7.

The underlying combinatorics appears to be closely connected to the theory of cluster algebras, specifically the cluster structure on the homogeneous coordinate ring of $\mathrm{Gr}(3, n+3)$: roughly, each spectral network corresponds to a cluster. For a brief account of this see §3.10, but there is much more to be understood here.

1.5. Non-simple zeroes

It would be very interesting to understand the generalization of Conjecture 1 when the zeroes of $P(z)$ are not required to be simple. In the case where exactly two zeroes collide, a generalization of the integral operator from Conjecture 1 written in [9] may be relevant. Indeed, the main example considered there ("pentagon example") is directly related to the case $n = 2$ of this paper.

1.6. Other ranks

There is a natural generalization of (1.1) to harmonic maps

$$g : \mathbb{C} \to \mathrm{SO}(K)\backslash \mathrm{SL}(K, \mathbb{R}), \tag{1.5}$$

[3] I abuse terminology by using "cross-ratio" for any $\mathrm{SL}(3, \mathbb{R})$-invariant function of the vertices of $Y(P)$.

again with a polynomial growth condition labeled by an integer n. In this case the maps g are labeled by *tuples* of polynomials $(P_2, P_3, \ldots, P_K)$, and the condition is that the roots of $\lambda^K + \sum_{i=2}^{K} \lambda^{K-i} P_i(z) = 0$ should behave locally as $\lambda_a \sim c_a z^{\frac{n}{K}}$ at large $|z|$, with a different constant $c_a \in \mathbb{C}$ for each root.[4,5] The asymptotic behavior of such a map should be controlled by a point of $\mathrm{Gr}_{\mathbb{R}}(K, n+K)/(\mathbb{R}^\times)^{n+K-1}$. Conjecture 1 should extend directly to this situation.

In the case $K = 2$ these harmonic maps have indeed been studied, e.g. in [12]. Moreover, the extension of Conjecture 1 to $K = 2$ is actually simpler than the case $K = 3$ which we treat in this paper. This is because the combinatorics of spectral networks in this case is easier: each spectral network gives a triangulation of the $(n+2)$-gon, and one reads off the cross-ratios X_γ directly from this triangulation. The necessary rules were worked out in [4].[6] Thus, it might have made sense to write this paper about $K = 2$ rather than $K = 3$. The main reason for choosing instead $K = 3$ is the accidental fact that the tools [1] were designed specifically for that case.

Working out concrete examples with $K > 3$, on the other hand, is likely infeasible without some improvement in our understanding of the combinatorics of spectral networks.

1.7. Real and complex Higgs bundles

One reason for our interest in Question 1 is that it is a special case (indeed, almost the simplest nontrivial case) of the *nonabelian Hodge correspondence* which relates Higgs bundles and flat connections:

[4]Strictly speaking, this is a generalization of our setup even when $K = 3$, since it allows two polynomials P_2, P_3 instead of just $P = P_3$, cf. (2.4). This generalization corresponds to taking general harmonic maps instead of minimal ones.

[5]Incidentally, when $K|n$, the constants $c_a \in \mathbb{C}$ have a global meaning, and varying them while holding them distinct should induce an action of the braid group B_K on the moduli space of flat irregular connections by "iso-Stokes deformation." The fact that such group actions can come from variation of parameters at irregular singularities has been emphasized by Philip Boalch; see e.g. [10] and references therein. It would be interesting to know whether this is the origin of the B_K action on $\mathrm{Gr}(K, rK)$ recently found in [11].

[6]Using these rules, an application of the $K = 2$ version of Conjecture 1 to a closely related problem, concerning minimal surfaces in AdS_3 with polygonal boundary, was already made in [13]. See also [14] where this was extended to a special case of minimal surfaces in AdS_5.

Question 2. *What can we say about the invariants of the flat* $\mathrm{SL}(K,\mathbb{R})$*-connection corresponding to a given rank* K *real Higgs bundle over a Riemann surface* C*, with or without singularities at points of* C*?*

Question 1 is the special case of Question 2 where we choose $K = 3$, $C = \mathbb{CP}^1$, fix a specific sort of irregular singularity at $z = \infty$, and restrict to Higgs bundles with $\mathrm{Tr}\,\varphi^2 = 0$. We explain this in §2.2. In turn, Question 2 is a special case of a similar question for general Higgs bundles and complex flat connections. A version of Conjecture 1 is expected to apply to these more general questions as well; this was the original context of [3, 4, 5].[7]

1.8. Hyperkähler metrics

Moduli spaces of (complex) Higgs bundles with irregular singularities, appropriately defined, are expected to carry natural hyperkähler metrics — generalizing the more familiar case of moduli spaces of Higgs bundles without singularities. In this paper, we do not explore these metrics. For context, though, we remark that the functions $\mathcal{X}_\gamma(\zeta)$ computed by the integral iteration in §4.1 are the main ingredient in a conjectural recipe for constructing these metrics, on the specific moduli spaces of Higgs bundles with irregular singularity appearing here; this recipe is described in [3]. The parameter ζ arises as the coordinate on the twistor sphere.

1.9. The WKB method

The problem of determining the large-P behavior of $Y(P)$ is part of a broader class of asymptotic problems which have been investigated at some length. I cannot really do this history justice, but at least some of the key references are:

- [16, 17, 18, 19, 20, 21, 22, 23] for Higgs bundles over a compact Riemann surface,
- [24, 12, 2] for harmonic maps $\mathbb{C} \to \mathrm{SO}(K)\backslash\mathrm{SL}(K,\mathbb{R})$ for $K = 2$ or $K = 3$,
- [25, 26] for opers over a compact Riemann surface.

[7] In sufficiently complicated cases — particularly the case of Higgs bundles without singularities — the WKB spectral networks are *dense* on C. This situation is more difficult, since problems of *dynamics* mix with the combinatorial problems. Some of the necessary tools in case $K = 2$ have been developed in [15].

A recurring theme in this area is the *WKB method* for studying families of flat connections,

$$\nabla(t) = t^{-1}\varphi + D + tA_1 + \cdots, \tag{1.6}$$

by studying flat sections in an expansion around $t = 0$. This is often applied taking $t = 1/R$, where R rescales the Higgs field or the polynomial P. It seems possible that the leading term in our asymptotic predictions, e.g. the aR in (1.3), could be obtained rigorously by a careful application of this technique, using the spectral network to organize the patching-together of local estimates. The work [19, 22], relating the spectral network to an asymptotic map to a building, seems to be connected to this picture.

One motivation of Conjecture 1, described in [4, 5], also involves the WKB method, but rather than taking $t = 1/R$ one considers a family of flat connections $\nabla(\zeta)$, $\zeta \in \mathbb{C}^\times$, associated to a *fixed* P, and takes $t = \zeta$. (The relevant family appears as (2.12) below.)

1.10. Quantum field theory

The original motivation of [3, 4, 5] was to address questions about BPS states in supersymmetric quantum field theories of "class S." The specific problem which we study here is related to the *(generalized) Argyres-Douglas theories* of *type* (A_2, A_{n-1}) in the taxonomy of [27]. The generalization mentioned in §1.6 similarly corresponds to type (A_{K-1}, A_{n-1}). The harmonic map equations are the equations giving Poincare invariant vacua for this theory formulated on $S^1 \times \mathbb{R}^3$, with the holonomies of electromagnetic gauge fields around S^1 chosen to be trivial.

2. Polynomials and polygons in $\mathbb{RP}^2$

2.1. A class of harmonic maps

We consider harmonic maps

$$g : \mathbb{C} \to \mathrm{SO}(3)\backslash\mathrm{SL}(3,\mathbb{R}). \tag{2.1}$$

Given such a g, the corresponding *Higgs field* is

$$\varphi = -(\partial_z \tilde{g}\tilde{g}^{-1})^+ \mathrm{d}z, \tag{2.2}$$

where $A^+ = \frac{1}{2}(A + A^t)$, and $\tilde{g}$ is any lift of g to $\mathrm{SL}(3,\mathbb{R})$. The harmonicity of g implies that φ is holomorphic. Thus if we define

$$\phi_2 = -\frac{1}{2}\operatorname{Tr}\varphi^2, \qquad \phi_3 = -\frac{1}{3}\operatorname{Tr}\varphi^3, \tag{2.3}$$

then ϕ_2, ϕ_3 are respectively holomorphic quadratic and cubic differentials on $\mathbb{C}$. In this paper we treat only the case of g for which

$$\phi_2 = 0, \qquad \phi_3 = P(z)\,\mathrm{d}z^3, \tag{2.4}$$

for P a polynomial of degree n, with complex coefficients.

The condition $\phi_2 = 0$ means that g is not only harmonic but also minimal [28]. For the purposes of this paper, this minimality is only indirectly relevant: our main reason for focusing on the case (2.4) is that it has been extensively studied in the recent [2]. We now briefly recall some facts established there; see [2] for a more detailed account and proofs.[8]

Theorem 1. *For any polynomial P there is a corresponding harmonic g for which (2.4) holds. This g is unique up to the action of $\mathrm{SL}(3,\mathbb{R})$ by isometries on the target.*

The harmonic g determines an $(n+3)$-tuple of points $y_r \in \mathbb{RP}^2$, as follows.[9] Write the leading term in $P(z)$ as μz^n for some $\mu \in \mathbb{C}^\times$. Fix a choice of root $\mu^{\frac{1}{n+3}}$. Then define $n+3$ rays $\ell_r \subset \mathbb{C}$ by

$$\ell_r = \mathrm{e}^{\frac{2\pi \mathrm{i} r}{n+3}} \mu^{-\frac{1}{n+3}} \mathbb{R}_+. \tag{2.5}$$

For $z \in \ell_r$ we have $\mu z^{n+3} \in \mathbb{R}_+$, so it admits a positive cube root, which we write $(\mu z^{n+3})^{\frac{1}{3}}$. One of the eigenvalues of $\tilde{g}(z)$ is asymptotically smallest, behaving as

$$\lambda \sim \exp\left(-\frac{3}{n+3}(\mu z^{n+3})^{\frac{1}{3}}\right) \tag{2.6}$$

as $z \to \infty$ along ℓ_r. The corresponding eigenspace of $\tilde{g}(z)$ limits to $y_r \in \mathbb{RP}^2$.

Theorem 2. *The y_r are the vertices of a convex $(n+3)$-gon in $\mathbb{RP}^2$.*

[8] In comparing our formulas with those of [2], $\frac{1}{2}C(z)_{\text{there}} = P(z)_{\text{here}}$.

[9] This description of the construction is different from that in [2], but produces the same y_r.

Recall that g is determined up to an overall $\mathrm{SL}(3,\mathbb{R})$ action from the right. This action transforms the y_r by an overall $\mathrm{SL}(3,\mathbb{R})$ action on $\mathbb{RP}^2$. Thus, for a given polynomial P, the y_r determine a convex $(n+3)$-gon in $\mathbb{RP}^2$ *up to* this $\mathrm{SL}(3,\mathbb{R})$ action. Now:

- Let $\mathcal{M}_{n+3} \subset (\mathbb{RP}^2)^{n+3}/\mathrm{SL}(3,\mathbb{R})$ denote the moduli space of convex $(n+3)$-gons with vertices labeled. When $n > 0$, $\mathcal{M}_{n+3}$ is a manifold, diffeomorphic to $\mathbb{R}^{2n-2}$.
- Let $\mathcal{P}_n$ be the space of pairs $(P, \mu^{\frac{1}{n+3}})$ where P is a degree n polynomial and $\mu^{\frac{1}{n+3}}$ is an $(n+3)$-rd root of the leading coefficient of P.

The passage from $(P, \mu^{\frac{1}{n+3}})$ to the y_r defines a map

$$Y : \mathcal{P}_n \to \mathcal{M}_{n+3}. \tag{2.7}$$

Both sides carry a natural action of $\mathbb{Z}/(n+3)\mathbb{Z}$; the map Y is equivariant for these actions.

Although we will not need this in what follows, we remark that Y is close to a homeomorphism, in the following sense. Y is invariant under affine-linear maps on $\mathcal{P}_n$,

$$(P(z), \mu^{\frac{1}{n+3}}) \mapsto (P(a^{n+3}z + b), \mu^{\frac{1}{n+3}} a^n), \qquad a \in \mathbb{C}^\times, b \in \mathbb{C}. \tag{2.8}$$

Thus Y descends to

$$\overline{Y} : \overline{\mathcal{P}}_n \to \mathcal{M}_{n+3} \tag{2.9}$$

where $\overline{\mathcal{P}}_n$ is the quotient of $\mathcal{P}_n$ by (2.8). For $n \geq 2$, it is shown in [2] that $\overline{Y}$ is a homeomorphism. A key building block of this result is a detailed theory of error estimates for the harmonic map equation (Wang's equation), previously developed in [29, 18, 28].

2.2. The nonabelian Hodge correspondence

In this section we explain how Y can be interpreted as a version of the *nonabelian Hodge correspondence* between Higgs bundles and flat complex connections. This is not strictly necessary for reading the rest of the paper, but provides some context.

The nonabelian Hodge correspondence originates from the celebrated work of Hitchin [30]. It was originally developed over a compact Riemann

surface C in [30, 31, 32, 33], and extended to the case of *tame ramification* (first-order poles on C) in [34]. We need the further extension to *wild ramification* (higher-order poles on C), developed in [35].

Briefly, the idea is as follows. We consider the holomorphic bundle $E = \mathcal{O}^{\oplus 3}$ over $\mathbb{CP}^1$, equipped with the meromorphic Higgs field

$$\varphi = \begin{pmatrix} 0 & 1 & 0 \\ 0 & 0 & 1 \\ -P(z) & 0 & 0 \end{pmatrix} \mathrm{d}z \quad \in \quad \mathrm{End}(E) \otimes K. \tag{2.10}$$

The pair (E, φ) is a Higgs bundle, with wild ramification at $z = \infty$. More precisely, we consider (E, φ) as a *good filtered Higgs bundle* in the language of [36], by assigning weights $(\alpha_1, \alpha_2, \alpha_3) = (\frac{n}{3}, 0, -\frac{n}{3})$ to the direct summands of E, and for a meromorphic section $s = (s_1, s_2, s_3)$ of E, defining $\nu_\infty(s) = \max\{\nu_\infty(s_i) + \alpha_i\}_{i=1}^3$, where $\nu_\infty(s_i) \in \mathbb{Z}$ is the ordinary order of singularity at $z = \infty$ of the meromorphic function s_i.[10]

We consider Hermitian metrics h in E, compatible with the filtration: this means that for any meromorphic section $s(z)$ of E, $h(s, s)$ scales like $|z|^{2\nu_\infty(s)}$ as $z \to \infty$. For any such h, let D_h denote the Chern connection in E, and $\varphi^{\dagger_h}$ the Hermitian adjoint of φ. The key analytic fact which we use is existence and uniqueness for *Hitchin's equations*, established in this context in [35]:[11]

Theorem 3. *There exists a Hermitian metric h in E, compatible with the filtration, with*

$$F_{D_h} + [\varphi, \varphi^{\dagger_h}] = 0. \tag{2.11}$$

This h is unique up to overall scalar multiple.

h is the *harmonic metric* associated to the Higgs bundle (E, φ).

We consider the family of complex connections in E given by

$$\nabla(\zeta) = \zeta^{-1}\varphi + D_h + \zeta\varphi^{\dagger_h}, \qquad \zeta \in \mathbb{C}^\times. \tag{2.12}$$

[10] The reason for the specific weights α_i given here is that they arrange that $\nu_\infty(\varphi(s))/\mathrm{d}z = \frac{n}{3} + \nu_\infty(s)$ for any meromorphic section s of E, which matches the singularity of the eigenvalues of φ, $\lambda \sim cz^{\frac{n}{3}}\mathrm{d}z$. Some more details of how the nonabelian Hodge correspondence works in this example appear in [37].

[11] More precisely, from the results of [35] one can directly deduce Theorem 3 in the case $3|n$. The extension to other n is believed to be straightforward, the basic mechanism being to pass to a cyclic covering, as described in [38] — see e.g. [36] for the statement, though I do not know a reference where all details have been explained.

The equation (2.11) implies that the connections $\nabla(\zeta)$ are all flat. From the fact that φ is traceless it follows that the harmonic metric h and flat connections $\nabla(\zeta)$ are compatible with the standard volume form on E. Thus each $\nabla(\zeta)$ is best thought of as a flat $\mathrm{SL}(3,\mathbb{C})$-connection over $\mathbb{CP}^1$, with an irregular singularity at $z=\infty$. There is also an extra symmetry around: if we define a bilinear pairing in E by

$$S = \begin{pmatrix} 0 & 0 & 1 \\ 0 & 1 & 0 \\ 1 & 0 & 0 \end{pmatrix} \in \mathrm{Hom}(E, E^*), \tag{2.13}$$

then

$$S^{-1}\varphi^T S = \varphi. \tag{2.14}$$

This extra symmetry makes (E,φ) into a *real Higgs bundle* as described in [39]: viewing h as a map $E \to \overline{E}^*$, we have the real structure $\tau = \overline{h}^{-1} \circ S : E \to \overline{E}$. Then

$$\overline{\nabla(\zeta)} = \overline{\zeta}^{-1}\overline{\varphi} + \overline{D_h} + \overline{\zeta\varphi^{\dagger_h}} = \tau^{-1} \circ \nabla(\overline{\zeta}^{-1}) \circ \tau. \tag{2.15}$$

When $|\zeta| = 1$ this becomes simply

$$\overline{\nabla(\zeta)} = \tau^{-1} \circ \nabla(\zeta) \circ \tau, \tag{2.16}$$

so using τ we can reduce $\nabla(\zeta)$ to an $\mathrm{SL}(3,\mathbb{R})$-connection in a real bundle $E_{\mathbb{R}}$.

The passage from the real Higgs bundle (E,φ) to the flat $\mathrm{SL}(3,\mathbb{R})$-connection $\nabla(\zeta=1)$ — using the harmonic metric h as intermediary — is the nonabelian Hodge correspondence for real Higgs bundles.

Now we want to relate this to the harmonic maps g described in §2.1. This just involves a slight shift in perspective, following [31, 32]. Let F denote the space of real flat sections for $\nabla(\zeta=1)$; F is a 3-dimensional real vector space with a natural volume element. Fix a basis $\{e_1, e_2, e_3\}$ of F, with unit volume. Also choose a real h-unitary trivialization of the bundle E away from $z=\infty$. Then let

$$\tilde{g}(z) = (e_1(z), e_2(z), e_3(z)) \in \mathrm{SL}(3,\mathbb{R}). \tag{2.17}$$

Changing the basis of F multiplies $\tilde{g}$ by a constant element of $\mathrm{SL}(3,\mathbb{R})$ on the right; changing the unitary trivialization of E multiplies $\tilde{g}$ by a smooth map

$\mathbb{C} \to \mathrm{SO}(3)$ on the left. Thus $\tilde{g}$ descends to a map $g : \mathbb{C} \to \mathrm{SO}(3)\backslash\mathrm{SL}(3,\mathbb{R})$, determined up to right-multiplication by an element of $\mathrm{SL}(3,\mathbb{R})$. This is the desired harmonic map.

Finally, we should explain how the polygons of §2.1 arise. From our present point of view they have to do with the behavior of the connection $\nabla(\zeta = 1)$ around the irregular singularity at $z = \infty$. The rays ℓ_r defined in (2.5) are anti-Stokes rays. Each ℓ_r determines a distinguished line in F, consisting of flat sections with the fastest asymptotic decay as $z \to \infty$: this gives the point y_r.

3. Background for the integral iteration

In this section we explain how to construct the input data needed in the formulation of Conjecture 1:

- parameters R, ϑ introduced in §3.1 below,
- a lattice Γ equipped with a *period map* Z and pairing $\langle \cdot, \cdot \rangle$, described in §3.2,
- *spectral coordinate* functions X_γ on $\mathcal{M}_{n+3}$, described in §3.5–§3.8,
- *BPS counts* $\Omega(P_0, \gamma) \in \mathbb{Z}$, described in §3.9.

In the process of constructing these data we will need the notion of *spectral network*, which we recall in §3.3–§3.4. The remaining §3.10 describes some relations between our constructions and cluster algebra.

3.1. Rescaling the cubic differential

From now on we take the polynomial P of the form

$$P(z) = R^3 \mathrm{e}^{-3\mathrm{i}\vartheta} P_0(z), \qquad R \in \mathbb{R}_+,\ \vartheta \in \mathbb{R}, \tag{3.1}$$

where $P_0(z)$ has only simple zeroes.

Of course, for a given $P(z)$ which we want to study, we could always set $R = 1$ and $\vartheta = 0$, by simply choosing $P_0(z) = P(z)$. Some reasons for our choice (3.1) are:

- later we will want to study the asymptotic behavior for large $P(z)$, which is conveniently formalized in the parameterization (3.1) as the $R \to \infty$ limit,
- solving the problem for a single value of ϑ turns out to give the solution for all ϑ at once, and so doing makes some of the structure more transparent.

3.2. The spectral curve, homology and periods

Our first fundamental player is the *spectral curve*, defined by the equation

$$\Sigma = \{x^3 + P_0(z) = 0\} \subset \mathbb{C}^2. \tag{3.2}$$

The projection map $\pi : (x, z) \mapsto z$ makes Σ a branched 3-fold cover of $\mathbb{C}$, with ramification points of index 3 over the n zeroes of $P_0(z)$. Using the Riemann-Hurwitz formula and looking at the branch structure around $z = \infty$ we compute

$$(\mathrm{genus}(\Sigma), \mathrm{holes}(\Sigma)) = \begin{cases} (n-2, 3) & \text{for } 3|n, \\ (n-1, 1) & \text{otherwise.} \end{cases} \tag{3.3}$$

We will make frequent use of the lattice

$$\Gamma = H_1(\Sigma, \mathbb{Z}), \tag{3.4}$$

which has

$$\mathrm{rank}(\Gamma) = 2n - 2. \tag{3.5}$$

Note that this formula is uniform in n, despite the case structure in (3.3). Also note a numerical "coincidence" which will be important later: $\mathrm{rank}(\Gamma) = \dim \mathcal{M}_{n+3}$.

Γ is equipped with the skew-symmetric intersection pairing $\langle \cdot, \cdot \rangle$, and the *period homomorphism*

$$Z : \Gamma \to \mathbb{C}, \qquad Z_\gamma = \oint_\gamma x \, \mathrm{d}z. \tag{3.6}$$

3.3. The WKB spectral network

Given (P_0, ϑ) there is a corresponding *WKB spectral network* $\mathcal{W}(P_0, \vartheta)$. Two examples of WKB spectral networks $\mathcal{W}(P_0, \vartheta)$ — the only two which we will consider in detail in this paper — are shown in Figures 7 and 11 below.

In the rest of this section we describe what $\mathcal{W}(P_0, \vartheta)$ is and how it is constructed. Our description uses the language of [5]; essentially the same

networks had been discovered earlier as *Stokes graphs*, e.g. [40, 41].[12]

The WKB spectral network is a collection of *WKB ϑ-trajectories*. A WKB ϑ-trajectory is a path $z(t)$ on $\mathbb{C}$, obeying a first-order ODE, depending on a choice of an ordered pair of distinct sheets of Σ lying over $z(t)$. We label these sheets as $(x_i(t), x_j(t))$ or sometimes just (i, j). The equation is:

$$(x_i(t) - x_j(t))\frac{\mathrm{d}z(t)}{\mathrm{d}t} = \mathrm{e}^{\mathrm{i}\vartheta}. \tag{3.7}$$

Note that (3.7) is invariant under the operation of simultaneously reversing $i \leftrightarrow j$ and $t \leftrightarrow -t$.

On any simply connected patch $U \subset \mathbb{C}$ with $P_0(z) \neq 0$ on U, the WKB ϑ-trajectories make up three foliations, labeled by the three choices of unordered pair (i, j); the three foliation leaves passing through each point meet at angles $2\pi/3$. Around a simple zero z_0 of $P_0(z)$ the structure is more interesting: there are 8 backward-inextendible WKB ϑ-trajectories which end on z_0; call these *critical trajectories*. See Figure 1.

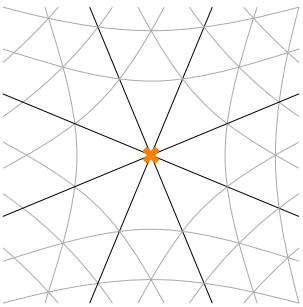

Figure 1: Some WKB ϑ-trajectories in a neighborhood of a simple zero of P_0 (orange cross). The critical trajectories are shown in black, others in gray.

[12]The networks described here may look surprising to a reader familiar with [5, 40, 41]; in those references the initial trajectories emanate from 3-valent vertices, while here we have 8-valent vertices. The reason for this difference is that we are studying a situation where all ramification points of Σ have index 3, while those earlier references mostly concerned ramification points of index 2. Had we chosen to study general harmonic maps as opposed to minimal ones, we would generically get ramification points of index 2, and our pictures would look more like those of [5, 40, 41]. The relation between these two situations is illustrated in Figure 36 of [5]. For a quick definition of the WKB spectral network in the more generic situation see Section 4.2 of [42].

The network $\mathcal{W}(P_0, \vartheta)$ is constructed as follows. We begin with the $8n$ critical trajectories emanating from the n zeroes of P_0, and extend them to $t \to +\infty$ by integrating the ODE (3.7). These trajectories will be included in $\mathcal{W}(P_0, \vartheta)$. Next we iteratively add more trajectories to $\mathcal{W}(P_0, \vartheta)$, as follows.

We consider intersections between trajectories already included in $\mathcal{W}(P_0, \vartheta)$. For each intersection there are three possibilities: either the trajectories meet head-on (in which case they actually coincide, differing only in their orientation and reversal of the sheet labels), they intersect in an angle $\frac{\pi}{3}$, or they intersect in an angle $\frac{2\pi}{3}$. For each intersection in angle $\frac{2\pi}{3}$ we add a new trajectory, as follows. The fact that the intersection angle is $\frac{2\pi}{3}$ implies that the labels of the intersecting trajectories are of the form $(i_1, j_1) = (i, j)$ and $(i_2, j_2) = (j, k)$. We add a new WKB ϑ-trajectory beginning from the intersection point, with the label (i, k), as shown in Figure 2.

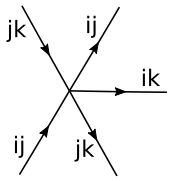

Figure 2: When two ϑ-trajectories in $\mathcal{W}(\vartheta, P_0)$ with labels $(i_1, j_1) = (i, j)$ and $(i_2, j_2) = (j, k)$ intersect, $\mathcal{W}(\vartheta, P_0)$ also includes a ϑ-trajectory carrying labels $(i_3, j_3) = (i, k)$, beginning at the intersection point.

As before, we extend these new trajectories to $t \to +\infty$. This may create new intersections between trajectories. We then repeat the process, letting these new intersections give birth to new trajectories, and so on. Define $\mathcal{W}(P_0, \vartheta)$ to be the full collection of trajectories produced in this fashion. *A priori* there is no reason this collection should be finite, but in the examples we study explicitly in §5 below, it is finite.

There is one phenomenon which requires extra attention: when we try to extend a trajectory in $\mathcal{W}(P_0, \vartheta)$ to $t \to +\infty$, it may run into a zero of P_0 at some finite t. In this case we say that (P_0, ϑ) is *BPS-ful*. The BPS-ful case is also the case in which there is at least one head-on collision between trajectories in $\mathcal{W}(P_0, \vartheta)$. If this does not happen then we say (P_0, ϑ) is *BPS-free*.

3.4. Asymptotics of WKB spectral networks

The behavior of $\mathcal{W}(P_0, \vartheta)$ near $z \to \infty$ is particularly simple. It is convenient to compactify to $\overline{\mathbb{C}} = \mathbb{C} \sqcup S^1$, introducing a "circle at infinity" (i.e. $\overline{\mathbb{C}}$ is the

oriented real blow-up of $\mathbb{CP}^1$ at $z = \infty$). There are $2n+6$ marked points on this circle, and each WKB ϑ-trajectory limits to one of these marked points.

Each marked point is labeled by an ordered pair of sheets (i, j) or more concisely ij, giving the label for all the WKB ϑ-trajectories asymptotic to that point. When we move from one marked point to the next (going around say counterclockwise) one label stays the same while the other changes, alternating between first and last: i.e. the labels on consecutive rays follow the pattern ij, ik, jk, ji, ki, kj, ... Again see Figure 7 and Figure 11 for illustrative examples.[13]

These marked points divide the circle at infinity into $2n+6$ arcs. Call an arc at infinity *initial* (*final*) if its two boundary points have the same initial (final) label; there are $n+3$ initial arcs and $n+3$ final arcs. Each of the asymptotic rays ℓ_r from (2.5) lies at the midpoint of one of the final arcs. Thus each ℓ_r can be labeled by the final label for the two nearest boundary rays; call this the *fading sheet* at ℓ_r.

This asymptotic structure is essentially universal: changing (P_0, ϑ) changes it only by an overall rotation of the circle at infinity.

3.5. Spectral coordinates

One of the predictions of [3, 4, 5] is that any BPS-free (P_0, ϑ) determines a coordinate system on $\mathcal{M}_{n+3}$.[14] More specifically, (P_0, ϑ) should determine for each $\gamma \in \Gamma$ a function $X_\gamma : \mathcal{M}_{n+3} \to \mathbb{R}^\times$, such that

$$X_{\gamma+\mu} = X_\gamma X_\mu, \tag{3.8}$$

and if we choose generators $\{\gamma_i\}_{i=1}^{2n-2}$ for Γ, the functions $\{X_{\gamma_i}\}_{i=1}^{2n-2}$ should give a coordinate system on $\mathcal{M}_{n+3}$. When (P_0, ϑ) is varied while remaining BPS-free, the functions X_γ should not change; when (P_0, ϑ) is varied across a BPS-ful locus, the X_γ may change.

[13] In comparing the asymptotics in those figures to the description above, one must keep in mind the permutations of sheets which occur when one crosses the branch cuts. For example, in Figure 7, starting from the rightmost marked point just above the branch cut, we see the sequence $31, 21, 23, 13, 12$; the next label would ordinarily be 32, but we also cross a branch cut which induces the permutation (123), so the next label is instead 13.

[14] Strictly speaking, what [3, 4, 5] predict is a *local* coordinate system on a patch of a *complexification* of $\mathcal{M}_{n+3}$, but it seems reasonable to conjecture that we get *global* coordinates after restricting to $\mathcal{M}_{n+3}$.

3.6. Abelianization trees

In this section and the next, we describe how the spectral coordinates X_γ are constructed using the spectral networks $\mathcal{W}(P_0, \vartheta)$.

Define an *abelianization tree compatible with* $\mathcal{W}(P_0, \vartheta)$ to be a collection of oriented arcs in $\overline{\mathbb{C}}$, with each arc labeled by a sheet of Σ and a representation of $\mathrm{SL}(3, \mathbb{R})$ (either fundamental V or its dual V^*), with the following properties:

- Each arc has two endpoints. The initial point of each arc may lie at one of the ℓ_r on the circle at infinity, or else lie at a junction as shown in Figure 3. The final point of each arc must lie at a junction.

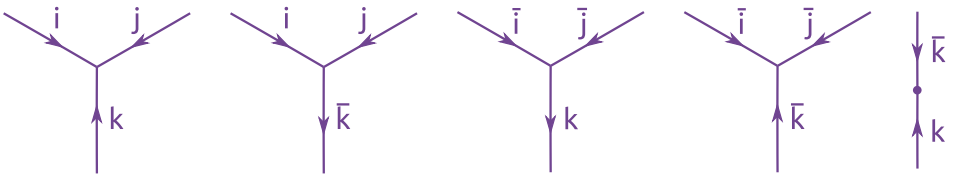

Figure 3: The types of junctions allowed in an abelianization tree. For the trivalent junctions i, j, k must all be distinct. If the sheet label carries an overbar, then the arc is carrying representation V^*, otherwise it is carrying representation V.

- If an arc ends at ℓ_r, then that arc carries the representation V, and its sheet label matches the fading sheet at ℓ_r (as defined in §3.4).
- Arcs of the abelianization tree do not cross one another.
- No arc carrying the label i and representation V crosses a trajectory of $\mathcal{W}(P_0, \vartheta)$ carrying a label (i, j).
- No arc carrying the label i and representation V^* crosses a trajectory of $\mathcal{W}(P_0, \vartheta)$ carrying a label (j, i).

Some examples of abelianization trees compatible with spectral networks appear in Figure 8 and Figure 12 below.

Dropping the sheet labels from an abelianization tree h induces a *tensor diagram* on $\overline{\mathbb{C}}$. This is a notion with a long history: see [43] for a very clear and precise review. This tensor diagram determines an $\mathrm{SL}(3, \mathbb{R})$-invariant map

$$A_h : V^{n+3} \to \mathbb{R}, \tag{3.9}$$

using the standard intertwiners

$$V \otimes V \otimes V \to \mathbb{R}, \quad V \otimes V \to V^*, \quad V^* \otimes V^* \to V, \\ V^* \otimes V^* \otimes V^* \to \mathbb{R}, \quad V \otimes V^* \to \mathbb{R}. \tag{3.10}$$

(We use the standard orientation of $\mathbb{C}$ to fix the orderings where needed.) A_h is homogeneous: its scaling weights under $(\mathbb{R}^\times)^{n+3}$ are the numbers of arcs ending at the $n+3$ marked points ℓ_r.

3.7. Combining abelianization trees for spectral coordinates

Now fix a formal linear combination of abelianization trees $\sum w_m h_m$, with weights $w_m \in \mathbb{Z}$, such that the total weighted number of arcs ending at each point ℓ_r is zero. Then the function

$$X = \prod_m A_{h_m}^{w_m} \tag{3.11}$$

is invariant under $(\mathbb{R}^\times)^{n+3}$, and so descends to $\mathcal{M}_{n+3} \subset (\mathbb{RP}^2)^{n+3}/\mathrm{SL}(3,\mathbb{R})$. X will be one of the spectral coordinates X_γ, for some $\gamma \in \Gamma$. It only remains to explain what γ is.

For this purpose, note each arc p of the abelianization tree h_m has a canonical lift to a 1-chain p^Σ on Σ: namely, if p is labeled by the sheet i, p^Σ is the lift of p to sheet i, with the orientation of p if p is carrying representation V, otherwise with the opposite orientation. Summing these lifts gives a singular 1-chain h_m^Σ for each abelianization tree h_m.

We now consider the 1-chain

$$c = \sum_m w_m h_m^\Sigma. \tag{3.12}$$

c is generally not closed, because of the trivalent junctions. However, the boundary ∂c is a 0-chain pulled back from the base $\overline{\mathbb{C}}$, so c becomes closed if we project to the quotient of the singular chain complex $C_*(\Sigma)$ by the subcomplex of chains pulled back from $\overline{\mathbb{C}}$. Moreover this projection is an isomorphism on homology, because $\overline{\mathbb{C}}$ is contractible. Thus c determines a class

$$\left[\sum_m w_m h_m^\Sigma\right] \in \Gamma. \tag{3.13}$$

Now we can finally state our definition of the spectral coordinate:

$$X_{[\sum_m w_m h_m^\Sigma]} = \prod_m A_{h_m}^{w_m}. \tag{3.14}$$

(3.14) defines X_γ for any $\gamma \in \Gamma$ which can be realized as $\gamma = \left[\sum_m w_m h_m^\Sigma\right]$ for some abelianization trees h_m and weights w_m. For this definition to be unambiguous, it must be true that every $\gamma \in \Gamma$ admits exactly one such realization. This is true in the examples we consider in §5 below. I do not know how generally it holds; in cases where it fails, we would have to resort to a more complicated construction of the X_γ, beginning from the notion of *abelianization* described in [5] and further reviewed in [42].

3.8. Asymptotic abelianization trees

For different choices of (P_0, ϑ) we get different compatible abelianization trees, and thus different spectral coordinates X_γ. However, as we have noted in §3.4, the structure of $\mathcal{W}(P_0, \vartheta)$ near $z = \infty$ is independent of (P_0, ϑ), up to an overall rotation of the plane. Thus any abelianization tree which lies entirely in the asymptotic region is in a sense universal, existing for every (P_0, ϑ). We call these *asymptotic abelianization trees*.

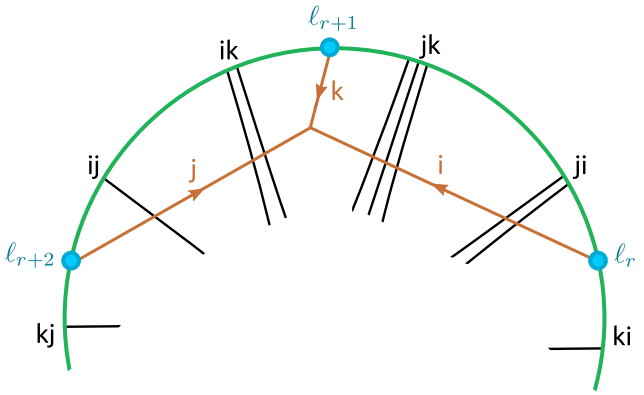

Figure 4: An asymptotic abelianization tree. Black lines represent WKB ϑ-trajectories in the asymptotic region of a WKB spectral network.

In Figure 4 we show an example of an asymptotic abelianization tree h, depending on a choice of $r \in \{1, \ldots, n+3\}$. The corresponding holonomy function is

$$A_h = p(r, r+1, r+2) \tag{3.15}$$

where $p(a,b,c)$ is a a "Plücker coordinate" depending on 3 of the v_i,

$$p(a,b,c) : (v_i)_{i=1}^{n+3} \mapsto \det(v_a, v_b, v_c). \tag{3.16}$$

3.9. BPS counts

The last ingredient we need is a collection of *BPS counts* $\Omega(P_0,\gamma) \in \mathbb{Z}$ for $\gamma \in \Gamma$. Here we describe one geometric approach to defining these counts. (This method is practicable for the simple examples we treat in §5, but for more elaborate examples it would be hard to use in practice. Thus we should mention that there are other ways, e.g. the *mutation method* [44, 45, 46] or the *spectrum generator / DT transformation* [4, 47, 48].)

Any WKB ϑ-trajectory p admits a canonical lift to a 1-chain p^Σ on Σ: namely, if p is labeled by the pair of sheets (i,j), p^Σ is the closure of the lift of p to sheet i, plus the orientation-reversal of the closure of the lift of p to sheet j. For $\gamma \in \Gamma$ a *finite web of charge* γ is a collection of trajectories p_l such that $\sum_l p_l^\Sigma$ is a compact 1-cycle in homology class γ. From the equation (3.7) it follows that if there is a finite web of charge γ inside a WKB spectral network $\mathcal{W}(P_0,\vartheta)$, then we must have $\vartheta = \arg Z_\gamma$. Moreover, in this case the network $\mathcal{W}(P_0,\vartheta)$ is BPS-ful in the sense of §3.3.

The desired $\Omega(P_0,\gamma)$ is a count of the finite webs of charge γ which occur inside the network $\mathcal{W}(P_0,\vartheta = \arg Z_\gamma)$. The meaning of the word "count" here is given by an algorithm explained in [5]. We will not describe this algorithm here, since in full generality it is a bit complicated; for the examples of §5 we only need some simple special cases, where the finite web is either a single critical trajectory connecting two zeroes of P_0 or a three-string junction: see Figure 5. In either of these cases, the algorithm in [5] says that the finite web contributes $+1$ to $\Omega(P_0,\gamma)$.

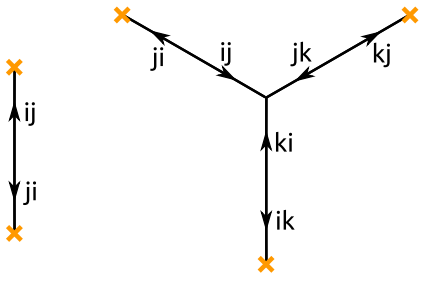

Figure 5: Two examples of finite webs.

A few final remarks about the BPS counts:

- For the examples of P_0 we consider in §5, there exist only finitely many $\gamma \in \Gamma$ for which $\Omega(P_0, \gamma) \neq 0$. We conjecture that this is always true for $n \leq 5$.
- The BPS counts have the symmetry property

$$\Omega(P_0, \gamma) = \Omega(P_0, -\gamma). \tag{3.17}$$

  To see this, note that $\mathcal{W}(P_0, \vartheta)$ and $\mathcal{W}(P_0, \vartheta + \pi)$ differ only by relabeling all trajectories $ij \to ji$, and thus any finite web in $\mathcal{W}(P_0, \vartheta)$ with charge γ has a partner in $\mathcal{W}(P_0, \vartheta + \pi)$ with charge $-\gamma$.
- Similarly, the $\Omega(P_0, \gamma)$ are invariant under the $\mathbb{Z}/3\mathbb{Z}$ action on Γ induced by the $\mathbb{Z}/3\mathbb{Z}$ action on Σ (cyclic permutation of sheets); this reflects the fact that $\mathcal{W}(P_0, \vartheta)$ and $\mathcal{W}(P_0, \vartheta + \frac{2\pi}{3})$ differ only by cyclic permutation of the sheet labels.
- The $\Omega(P_0, \gamma)$ are expected to be examples of *generalized Donaldson-Thomas invariants* in the sense of Kontsevich-Soibelman / Joyce-Song [49, 50]. In particular, the collection $\{\Omega(P_0, \gamma)\}_{\gamma \in \Gamma}$ depends on P_0 in a piecewise constant fashion; it can jump where P_0 crosses a *wall of marginal stability* in the space of polynomials. These jumps are governed by the Kontsevich-Soibelman wall-crossing formula [49, 3, 5].
- A related fact is that, when (P_0, ϑ) cross a BPS-ful locus, the jump of the spectral coordinates X_γ is determined by the $\Omega(P_0, \gamma)$ for those γ such that $Z_\gamma e^{-i\vartheta} \in \mathbb{R}_-$.

3.10. Spectral coordinates as cluster coordinates

This section describes an interpretation of the functions A_h associated to abelianization trees in the language of cluster algebra. It is not strictly necessary for the rest of the paper. See [43] for much more on the cluster structures we use here, and their relation to tensor diagrams.

Let $\mathcal{C}_{n+3}$ denote the coordinate ring of $V^{n+3}/\mathrm{SL}(3, \mathbb{R})$. This ring is a classic example of a *cluster algebra*, as first described in [51]. This structure picks out a collection of distinguished *clusters* in $\mathcal{C}_{n+3}$: these are collections of *cluster* $\mathfrak{A}$*-variables* $\{a_m\}_{m=1}^{3n+1}$, where the first $2n-2$ are called *unfrozen* and depend on the choice of cluster, and the last $n+3$ are *frozen* and are common to all clusters.

The reason for discussing the clusters here is the following: there seems to be a correspondence between clusters and spectral networks (as anticipated in [5].) Namely, given a spectral network $\mathcal{W}$, the functions A_h realized

by abelianization trees compatible with $\mathcal{W}$ are often the monomials in the cluster $\mathfrak{A}$-variables of some cluster in $\mathcal{C}_{n+3}$. This is true for every spectral network $\mathcal{W}(P_0, \vartheta)$ I have examined (with $n = 2, 3$). I conjecture that it is true for all spectral networks $\mathcal{W}(P_0, \vartheta)$ for BPS-free (P_0, ϑ) when $n \leq 5$.[15] It would be very interesting to understand the relation between this proposal and the results in [43], and to develop an efficient method of mapping the spectral networks to the clusters.

In this correspondence, the $n + 3$ asymptotic abelianization trees described in §3.8 give the $n + 3$ frozen variables, which are the Plücker coordinates (3.15). In the language of [43] these are *special invariants*. Non-asymptotic abelianization trees give the $2n - 2$ unfrozen variables. Some of these unfrozen variables are also Plücker coordinates $p(a, b, c)$, now with a, b, c not consecutive. For example, when $n = 2$, all cluster $\mathfrak{A}$-variables are Plücker coordinates. The first example of a cluster $\mathfrak{A}$-variable which is not a Plücker coordinate arises for $n = 3$; we will encounter it in §5.3 below (see (5.16)).

The cluster structures we discussed above are closely related to ones introduced in [52], which were very important in the original developments leading to [5] and Conjecture 1. However, as far as I understand, the cluster structures we are now considering are not *quite* examples of the formalism in [52]: that formalism does include moduli spaces of flat connections with irregular singularity, but a different sort of irregular singularity than we need here, which leads to moduli spaces involving complete flags rather than lines.

4. The integral iteration and its consequences

We can now give the sharp formulation of Conjecture 1 and some consequences.

4.1. The integral iteration

In this section we formulate Conjecture 1 precisely. Concretely, we give a conjectural way of computing the point $Y(P) \in \mathcal{M}_{n+3}$, in the spectral coordinate system X_γ on $\mathcal{M}_{n+3}$ associated to (P_0, ϑ).[16]

[15] These are the cases for which $\mathcal{C}_{n+3}$ has only finitely many clusters [51].

[16] Of course, once we have determined the coordinates of $Y(P)$ in one coordinate system on $\mathcal{M}_{n+3}$ we can then change coordinates to any other; nevertheless, Conjecture 1 is most naturally phrased as a recipe which produces specifically the spectral coordinates X_γ.

Although our aim is to compute *numbers* X_γ, the strategy is first to construct *functions* $\mathcal{X}_\gamma(\zeta)$ of a parameter $\zeta \in \mathbb{C}^\times$, as follows. We begin with $\mathcal{X}_\gamma^{(0)}(\zeta) = 0$ and then define inductively[17]

$$\mathcal{X}_\gamma^{(k+1)}(\zeta) = \exp\Bigg[R(\zeta^{-1}Z_\gamma + \zeta\overline{Z}_\gamma) + \frac{1}{4\pi\mathrm{i}}\sum_{\mu\in\Gamma}\Omega(P_0,\mu)\langle\gamma,\mu\rangle\int_{Z_\mu\mathbb{R}_-}\frac{\mathrm{d}\zeta'}{\zeta'}\frac{\zeta'+\zeta}{\zeta'-\zeta}\log(1+\mathcal{X}_\mu^{(k)}(\zeta'))\Bigg]. \tag{4.1}$$

The desired functions are obtained in the limit:

$$\mathcal{X}_\gamma(\zeta) = \lim_{k\to\infty}\mathcal{X}_\gamma^{(k)}(\zeta). \tag{4.2}$$

A sketch of an argument for the existence of this limit at sufficiently large R can be found in [3]. For our purposes in this paper we take the convergence as a working assumption. Finally, to recover the desired numbers X_γ, we specialize:

$$X_\gamma = \mathcal{X}_\gamma(\zeta = \mathrm{e}^{\mathrm{i}\vartheta}). \tag{4.3}$$

The equations (4.1), (4.2), (4.3), together with the definitions of symbols given in §3, make up the precise form of Conjecture 1.

A few remarks:

- The right side of (4.3) is real, as it should be, while $\mathcal{X}_\gamma(\zeta)$ is generally complex for $|\zeta| \neq 1$. The proof that $\mathcal{X}_\gamma(\zeta = \mathrm{e}^{\mathrm{i}\vartheta})$ is real uses the symmetry property (3.17).
- The $\mathcal{X}_\gamma(\zeta)$ depend on ζ in a *piecewise* holomorphic fashion, jumping whenever ζ crosses the contours of integration in (4.1), i.e. the rays $Z_\mu\mathbb{R}_-$ with $\Omega(P_0,\mu) \neq 0$ and $\langle\mu,\gamma\rangle \neq 0$. This means that the X_γ we compute from (4.3) depend discontinuously on ϑ. Of course, the polygon $Y(P) \in \mathcal{M}_{n+3}$ depends continuously on ϑ. The jumps of X_γ just reflect the fact that the spectral coordinate system on $\mathcal{M}_{n+3}$ which we use jumps when ϑ crosses a BPS-ful phase.

[17] In (4.1) the factor $\log(1+\mathcal{X}_\mu(\zeta'))$ appears. In the general formalism of [3] one would expect to see instead $\log(1-\sigma(\mu)\mathcal{X}_\mu(\zeta'))$ for some $\sigma : \Gamma \to \{\pm 1\}$. In the examples of this paper we always have $\sigma(\mu) = -1$ whenever $\Omega(P_0,\mu) \neq 0$, so we have simplified by making this substitution.

- The $\mathcal{X}_\gamma(\zeta)$ for general ζ do have an interpretation, most easily expressed in the language of §2.2: they are the spectral coordinates of the family of connections (2.12).

4.2. Exact consequences

Now let us describe some consequences of Conjecture 1.

One important special case arises when γ lies in the kernel of the pairing $\langle\cdot,\cdot\rangle$. (Recall from §3.2 that this kernel is nontrivial only when $3|n$.) In this case the coefficients of the integrals in (4.1) vanish, and (4.2) becomes the exact prediction

$$\mathcal{X}_\gamma(\zeta) = \exp\left[R(\zeta^{-1}Z_\gamma + \zeta\overline{Z}_\gamma)\right], \tag{4.4}$$

giving after the substitution (4.3)

$$X_\gamma = \exp\left(a_\gamma R\right), \tag{4.5}$$

with

$$a_\gamma = 2\,\mathrm{Re}(\mathrm{e}^{-\mathrm{i}\vartheta}Z_\gamma). \tag{4.6}$$

4.3. Asymptotic consequences for $R \to \infty$

The more interesting case is that of γ *not* in the kernel of the pairing $\langle\cdot,\cdot\rangle$. Then (4.2) does not reduce to a simple exact formula for the spectral coordinate X_γ. Nevertheless, we can extract asymptotic formulas in the limit $R \to \infty$. For this purpose define

$$\alpha_\mu = -\frac{Z_\mu}{|Z_\mu|} \tag{4.7}$$

and assume for simplicity that, for all $\mu \in \Gamma$ such that $\Omega(P_0,\mu) \neq 0$, we have $\zeta \neq \alpha_\mu$. We consider the integral equation obeyed by $\mathcal{X}_\gamma(\zeta)$ (obtained by setting $k = \infty$ in (4.1)) and make a self-consistent analysis: assume that the integral terms are exponentially small in the $R \to \infty$ limit, use this assumption to replace $\mathcal{X}_\mu(\zeta')$ by $\exp R(\zeta'^{-1}Z_\mu + \zeta'\overline{Z}_\mu)$ in the integral, then evaluate the $R \to \infty$ asymptotics of the integral by the saddle point method.

This leads to the following prediction. Write

$$\mathcal{X}_\gamma(\zeta) = \exp\left[(\zeta^{-1}Z_\gamma + \zeta\overline{Z}_\gamma)R + \sum_{\mu\in\Gamma} \frac{\Omega(P_0,\mu)\langle\gamma,\mu\rangle}{4\pi\mathrm{i}} \frac{\alpha_\mu+\zeta}{\alpha_\mu-\zeta}\sqrt{\frac{\pi}{R|Z_\mu|}}\mathrm{e}^{-2|Z_\mu|R}\right. \tag{4.8}$$

$$+ \delta(R,\zeta)\Big],$$

for some "remainder" $\delta(R,\zeta)$.[18] We predict that

$$\lim_{R\to\infty} \sqrt{R}\mathrm{e}^{2\rho R}\delta(R,\zeta) = 0, \tag{4.9}$$

where

$$\rho = \min\left\{|Z_\mu| : \mu\in\Gamma,\ \Omega(P_0,\mu)\langle\gamma,\mu\rangle \neq 0\right\}. \tag{4.10}$$

Said otherwise: as $R\to\infty$, the leading behavior of $\log\mathcal{X}_\gamma$ is of order R; the first correction is exponentially smaller, of order $\frac{1}{\sqrt{R}}\mathrm{e}^{-2\rho R}$; both terms are captured by the explicit formula (4.8).

Making the substitution (4.3) in (4.8) we get $R\to\infty$ asymptotics for the spectral coordinate X_γ:

$$X_\gamma = \exp\left[a_\gamma R + \sum_{\mu\in\Gamma}\frac{\Omega(P_0,\mu)\langle\gamma,\mu\rangle}{4\pi\mathrm{i}}\frac{\alpha_\mu+\mathrm{e}^{\mathrm{i}\vartheta}}{\alpha_\mu-\mathrm{e}^{\mathrm{i}\vartheta}}\sqrt{\frac{\pi}{R|Z_\mu|}}\mathrm{e}^{-2|Z_\mu|R} + \delta(R,\mathrm{e}^{\mathrm{i}\vartheta})\right], \tag{4.11}$$

with a_γ again given by (4.6).

5. Examples

In this final section we work out the detailed statement of Conjecture 1 for two examples of polynomials $P_0(z)$.

5.1. An $n = 2$ example (pentagon)

We first consider a degree 2 example,

$$P_0(z) = \frac{1}{2}\left(-z^2+1\right). \tag{5.1}$$

The spectral curve Σ defined in (3.2) is a 3-sheeted cover of $\mathbb{C}$, with ramification points of index 3 over $z=\pm1$. Σ is a one-holed torus. Thus Γ is a lattice of rank 2, with nondegenerate intersection pairing. In Figure 6 we show a convenient choice of generators γ_1,γ_2 with $\langle\gamma_1,\gamma_2\rangle = 1$.

[18] The values $\delta(R,\zeta)=\pm\infty$ are allowed, but our claim (4.9) implies that there is some R_0 such that $\delta(R,\zeta)$ is finite for $R>R_0$.

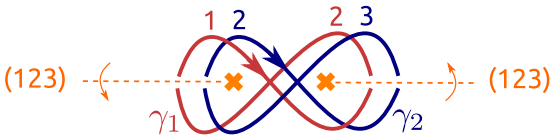

Figure 6: Generators γ_1, γ_2 for $\Gamma = H_1(\Sigma, \mathbb{Z})$, where P_0 is given by (5.1). Σ is shown as a triple cover of $\mathbb{C}$, with ramification points at $z = \pm 1$ (orange crosses). The cover is trivialized away from branch cuts (dashed lines). Crossing a branch cut in the direction indicated by the arrow induces the permutation (123) of sheet labels. The numerical labels next to paths indicate which sheet of Σ the paths lie on.

The corresponding period integrals (3.6) can be computed in closed form to give

$$Z_{\gamma_1} = \mathrm{e}^{5\pi \mathrm{i}/6} \left(\frac{12 \times 2^{2/3} \times \pi^{3/2}}{5\Gamma\left(-\frac{1}{6}\right)\Gamma\left(\frac{2}{3}\right)} \right), \qquad Z_{\gamma_2} = \mathrm{e}^{2\pi \mathrm{i}/3} Z_{\gamma_1}, \tag{5.2}$$

or numerically

$$Z_{\gamma_1} \approx -2.00324 + 1.15657\mathrm{i}, \qquad Z_{\gamma_2} \approx -2.31315\mathrm{i}. \tag{5.3}$$

The analysis of spectral networks in this case (see §5.2) leads to the following:

- For $|\vartheta| < \frac{\pi}{6}$, the spectral coordinates attached to the network $\mathcal{W}(P_0, \vartheta)$ are

  $$X_{\gamma_1} = \frac{p(1,2,3)p(3,4,5)}{p(1,3,5)p(2,3,4)}, \qquad X_{\gamma_2} = \frac{p(1,3,5)p(2,3,4)p(1,2,5)}{p(1,2,3)p(2,3,5)p(1,4,5)}, \tag{5.4}$$

  where we have labeled the rays ℓ_r as in Figure 7 below, and we recall the definition of Plücker coordinates

  $$p(a,b,c) : (v_i)_{i=1}^{n+3} \mapsto \det(v_a, v_b, v_c). \tag{5.5}$$

- The BPS counts are:

  $$\Omega(P_0, \gamma) = \begin{cases} 1 & \text{for } \pm\gamma \in \{\gamma_1, \gamma_2, \gamma_1 + \gamma_2\}, \\ 0 & \text{otherwise.} \end{cases} \tag{5.6}$$

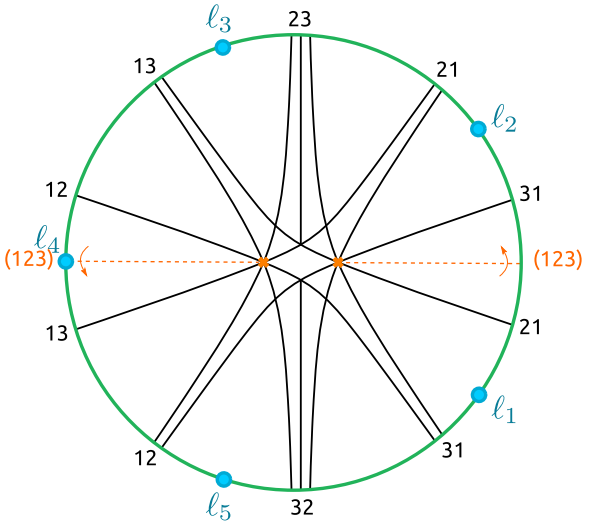

Figure 7: The spectral network $\mathcal{W}(P_0, \vartheta = 0)$ where P_0 is given in (5.1). It consists of 18 WKB ϑ-trajectories in all: 16 critical trajectories emanating from the zeroes of P_0, and 2 more born from intersection points. These 18 trajectories approach 10 asymptotic directions, equally spaced around the circle at infinity.

This is all the data necessary to formulate Conjecture 1 and its consequences as described in §4. In particular, specializing the statements of §4.3 to this example we get predictions for the $R \to \infty$ asymptotics of the X_γ. To give one concrete such prediction, we specialize to $\vartheta = 0$ and choose $\gamma = \gamma_1$. Then (4.11) becomes

$$\frac{p(1,2,3)p(3,4,5)}{p(1,3,5)p(2,3,4)} = \exp\left(aR - \frac{3}{2\sqrt{\pi\rho R}}\mathrm{e}^{-2\rho R} + \delta(R)\right), \tag{5.7}$$
$$a \approx -4.00648, \quad \rho \approx 2.31315,$$

where the remainder function $\delta(R)$ obeys

$$\lim_{R\to\infty} \delta(R)\sqrt{R}\mathrm{e}^{2\rho R} = 0. \tag{5.8}$$

5.2. Spectral network analysis for the $n = 2$ example

In this section we sketch the spectral network analysis leading to (5.4) and (5.6).

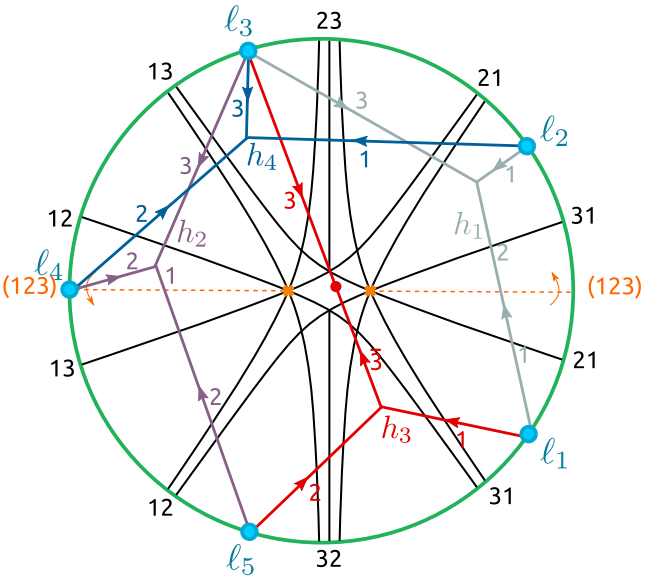

Figure 8: Four abelianization trees on the spectral network $\mathcal{W}(P_0, \vartheta = 0)$ where P_0 is given in (5.1).

We begin with the spectral coordinate formulas (5.4). For this purpose we need to draw the network $\mathcal{W}(P_0, \vartheta = 0)$; it is shown in Figure 7, obtained using the Mathematica code [53].[19] Then, according to the rules explained in §3.5, we need to draw the abelianization trees compatible with this network. In Figure 8 we show four abelianization trees h_m. h_1, h_2 and h_4 are asymptotic abelianization trees (cf. Figure 4), while h_3 is not asymptotic: the legs labeled 3 and $\overline{3}$ pass through the middle of the spectral network. It is instructive to see why h_3 is compatible with the spectral network: the key point is that the leg labeled 3 does not cross any trajectory labeled 31 or 32 (it does cross trajectories labeled 13, 23, and 21), and the leg labeled $\overline{3}$ does not cross any trajectory labeled 13 or 23 (it does cross ones labeled 32, 31, and 12).

The functions attached to these abelianization trees are

(5.9)
$$A_{h_1} = p(1,2,3), \quad A_{h_2} = p(3,4,5), \quad A_{h_3} = p(1,3,5), \quad A_{h_4} = p(2,3,4).$$

[19] A version of this code is included with the arXiv version of this paper, as `swn-plotter.nb`.

Combining these trees according to the rules of §3.6, with weights $w_1 = w_2 = +1$, $w_3 = w_4 = -1$, we get a closed cycle which turns out to be γ_1. Thus we have

$$X_{\gamma_1} = \frac{p(1,2,3)p(3,4,5)}{p(1,3,5)p(2,3,4)} \tag{5.10}$$

as we claimed in (5.4). A similar construction involving 6 abelianization trees gives X_{γ_2}.

In this way we obtain the formulas (5.4) for $\vartheta = 0$. It still remains to see why these formulas also hold for other ϑ with $|\vartheta| < \frac{\pi}{6}$. The reason is that the X_γ are invariant under variations of ϑ, so long as we do not cross a phase which is BPS-ful. (Concretely, such variations of ϑ deform $\mathcal{W}(P_0, \vartheta)$ in a way which does not affect the set of compatible abelianization trees.) By drawing the networks $\mathcal{W}(P_0, \vartheta)$ for various phases ϑ one can spot by eye the phases which are BPS-ful: these are $\vartheta = \pm\frac{\pi}{6}, \pm\frac{\pi}{2}, \pm\frac{5\pi}{6}$.[20]

The BPS-ful phases are also relevant for another reason: we use them in the process of determining the BPS counts (5.6), following the rules of §3.9. At each of the BPS-ful phases a single finite web appears in $\mathcal{W}(P_0, \vartheta)$, consisting of a single trajectory connecting the two zeroes of P_0. For example, in Figure 9 we show the network $\mathcal{W}(P_0, \vartheta)$ very near $\vartheta = -\frac{\pi}{6}$. Note the two trajectories which almost meet head-to-head in the center of the picture. At $\vartheta = -\frac{\pi}{6}$ these two merge into a single trajectory p, whose lift p^Σ is in homology class $-\gamma_1$. According to the rules described in §3.9, this trajectory is responsible for a nonzero count, $\Omega(P_0, -\gamma_1) = 1$. (Note this is consistent with the fact that $\arg Z_{-\gamma_1} = -\frac{\pi}{6}$.) Looking similarly at the other BPS-ful phases we get the BPS counts (5.6).

5.3. An $n = 3$ example (hexagon)

Next we consider the degree 3 case

$$P_0 = \frac{1}{2}\left(-z^3 + 3z^2 + 2\right). \tag{5.11}$$

In this case the spectral curve Σ defined in (3.2) is a 3-sheeted cover of $\mathbb{C}$, with ramification points of index 3 over the 3 zeroes of P_0. Σ is a 3-holed

[20] A movie containing pictures of the networks $\mathcal{W}(P_0, \frac{n\pi}{300})_{n=0}^{99}$ is included with the arXiv version of this paper, as `pentagon.gif`. (Recall that a shift $\vartheta \to \vartheta + \frac{\pi}{3}$ can be compensated by a relabeling of the walls of $\mathcal{W}(P_0, \vartheta)$, so we need not explore phases beyond $[0, \frac{\pi}{3})$.)

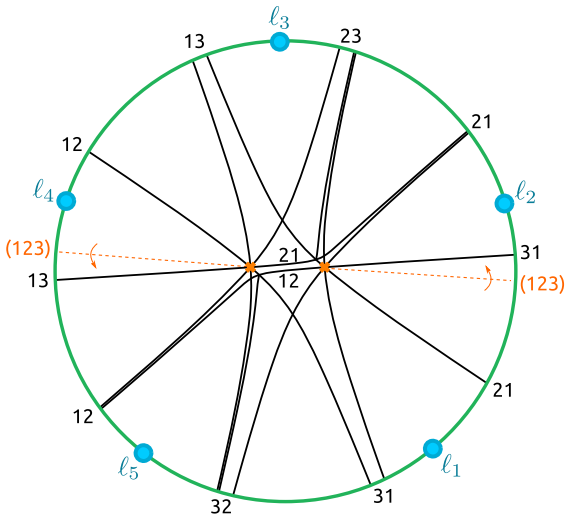

Figure 9: The spectral network $\mathcal{W}(P_0, \vartheta = -\frac{\pi}{6} + 0.1)$ where P_0 is given in (5.1). This picture can be reached by a continuous deformation of Figure 7, realized concretely by the family of BPS-free networks $\mathcal{W}(P_0, \vartheta)$ with ϑ varying from 0 to $-\frac{\pi}{6} + 0.1$.

torus. Thus Γ is a lattice of rank 4, with intersection pairing of rank 2. In Figure 10 we show a convenient choice of generators, with $\langle \gamma_1, \gamma_2 \rangle = 1$ and γ_3, γ_4 in the kernel of $\langle \cdot, \cdot \rangle$. The numerically computed periods are

(5.12)
$$(Z_{\gamma_i})_{i=1}^4 \approx (2.30298,\ 5.47033 + 4.48792\mathrm{i},\ -4.31884 + 2.49348\mathrm{i},\ -4.98697\mathrm{i}).$$

The analysis of spectral networks in this case (see §5.4) leads to the following:

- We have, using the basis $(\gamma_i)_{i=1}^4$ for Γ,

  (5.13)
  $$\Omega(P_0, \gamma) = \begin{cases} 1 & \text{if } \pm\gamma \in \left\{ \begin{array}{l} (1,0,0,0),\ (0,-1,-1,-1),\ (-1,1,1,1), \\ (0,1,0,0),\ (1,-1,-1,0),\ (-1,0,1,0), \\ (0,-1,-1,0),\ (1,0,-1,-1),\ (-1,1,2,1), \\ (1,1,0,0),\ (1,-2,-2,-1),\ (-2,1,2,1) \end{array} \right\}, \\ 0 & \text{otherwise.} \end{cases}$$

- For $0 < \vartheta < 0.36$, the spectral coordinates attached to the network

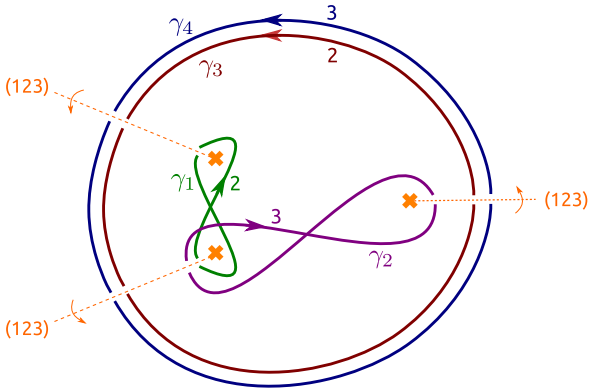

Figure 10: Generators $\{\gamma_i\}_{i=1}^4$ for $\Gamma = H_1(\Sigma, \mathbb{Z})$, where P_0 is given by (5.11). The notation is as in Figure 6.

$\mathcal{W}(P_0, \vartheta)$ are

$$X_{\gamma_1} = \frac{q(2,3,4,5,6,1)}{p(1,5,6)p(2,3,4)}, \quad X_{\gamma_2} = \frac{p(1,5,6)p(2,3,6)p(1,4,6)}{p(1,2,6)p(1,3,6)p(4,5,6)}, \tag{5.14}$$

$$X_{\gamma_3} = \frac{p(1,2,3)p(4,5,6)}{p(2,3,4)p(1,5,6)}, \quad X_{\gamma_4} = \frac{p(1,2,6)p(3,4,5)}{p(1,2,3)p(4,5,6)}. \tag{5.15}$$

Here in addition to the Plücker coordinates $p(a, b, c)$ we use the invariant (called "hexapod invariant" in [43])

$$q(a,b,c,d,e,f) : (v_i)_{i=1}^{n+3} \mapsto \det(v_a \times v_b, v_c \times v_d, v_e \times v_f). \tag{5.16}$$

This is all the data necessary to formulate Conjecture 1 and its consequences as described in §4. Unlike the case of §5.1 above, here we get some *exact* predictions, as described in §4.2: indeed, since γ_3 and γ_4 are in the kernel of $\langle \cdot, \cdot \rangle$ we get exact formulas for X_{γ_3} and X_{γ_4}. For example, suppose we specialize to $\vartheta = 0.2$ and choose $\gamma = \gamma_3$. Then (4.5) becomes

$$\frac{p(1,2,3)p(4,5,6)}{p(2,3,4)p(1,5,6)} = \exp(aR), \quad a \approx -7.4748. \tag{5.17}$$

We also get asymptotic predictions for the other coordinates, as we did in §5.1 above. For example, specializing to $\vartheta = 0.2$ and $\gamma = \gamma_1$, (4.11) becomes

$$\frac{q(2,3,4,5,6,1)}{p(1,5,6)p(2,3,4)} = \exp\left(aR + \frac{c}{\sqrt{R}} e^{-2\rho R} + \delta(R)\right) \tag{5.18}$$

where

$$a \approx 4.5142, \quad \rho \approx 2.3030, \quad c \approx 0.1961, \tag{5.19}$$

and the remainder function $\delta(R)$ obeys

$$\lim_{R\to\infty} \delta(R)\sqrt{R}\mathrm{e}^{2\rho R} = 0. \tag{5.20}$$

5.4. Spectral network analysis for the $n = 3$ example

In this section we sketch the spectral network analysis leading to (5.13), (5.14), (5.15). This is parallel to §5.2 above.

The spectral coordinates (5.14), (5.15) are obtained as follows. We first draw the network $\mathcal{W}(P_0, \vartheta = 0.1)$, shown in Figure 11, obtained using [53]. Then, we draw compatible abelianization trees. In Figure 12 we show three

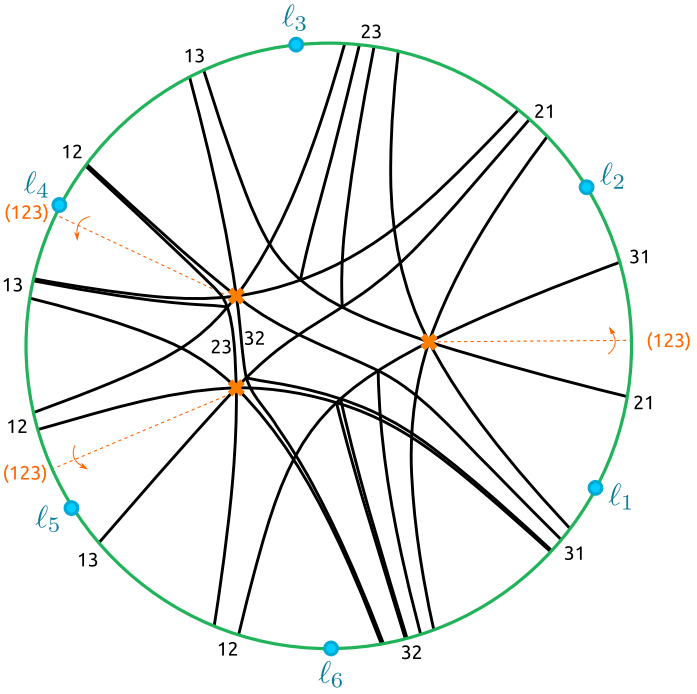

Figure 11: The spectral network $\mathcal{W}(P_0, \vartheta = 0.1)$ where P_0 is given in (5.11). It consists of 31 WKB ϑ-trajectories: 24 critical trajectories emanating from the zeroes of P_0, and 7 more born from intersection points.

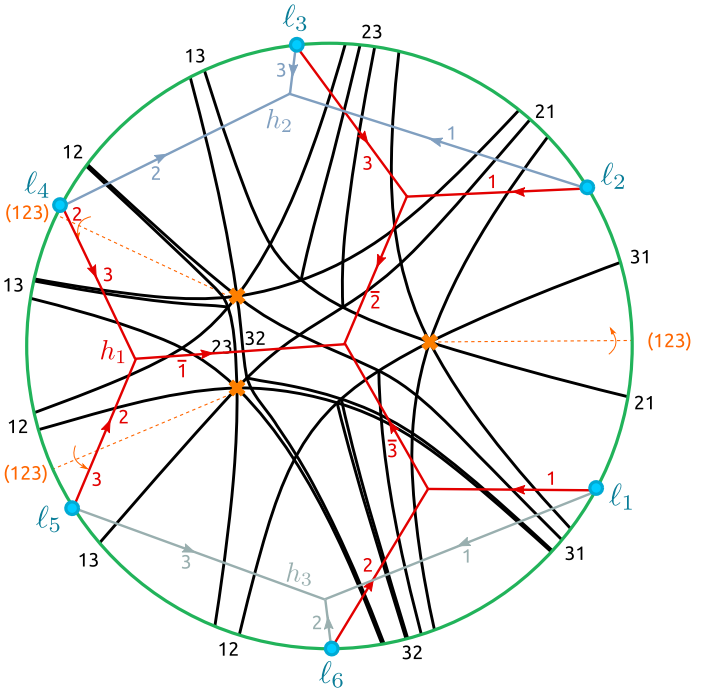

Figure 12: Three abelianization trees compatible with the spectral network $\mathcal{W}(P_0, \vartheta = 0.1)$ where P_0 is given in (5.11).

abelianization trees h_m. h_2 and h_3 are asymptotic abelianization trees (cf. Figure 4) while h_1 is not. h_1 is a more interesting tree than we have seen thus far: it is a "hexapod" in the terminology of [43]. The functions attached to these abelianization trees are

$$A_{h_1} = q(2,3,4,5,6,1), \qquad A_{h_2} = p(1,5,6), \qquad A_{h_3} = p(2,3,4). \tag{5.21}$$

Combining these according to the rules of §3.6, with weights $w_1 = +1$, $w_2 = w_3 = -1$, we get a closed cycle which turns out to be γ_1. Thus we have

$$X_{\gamma_1} = \frac{q(2,3,4,5,6,1)}{p(1,5,6)p(2,3,4)} \tag{5.22}$$

as we claimed in (5.14). Similar constructions and computations give the other X_{γ_i} of (5.14), (5.15).

The BPS-ful phases and the BPS counts $\Omega(P_0, \gamma)$ in (5.13) were determined, as in the $n = 2$ case above, by direct examination of the networks

$\mathcal{W}(P_0, \vartheta)$ as ϑ varies.[21] For each unordered pair (z, z') of zeroes of P_0, we find 6 finite BPS webs which are single trajectories connecting z to z'. For example, at $\vartheta = 0$ we get a finite BPS web of charge γ_1, connecting the two leftmost zeroes; indeed, in Figure 11 one can easily see two trajectories in $\mathcal{W}(P_0, \vartheta = 0.1)$ which almost meet head-on, and which do meet head-on when ϑ is adjusted from 0.1 to 0. Similarly, at $\vartheta \approx 0.36$ we get a finite BPS web of charge $\gamma_1 - \gamma_3 - \gamma_4$, consisting of a single trajectory connecting the zeroes at top left and at right. There are also 6 more finite BPS webs which are three-string junctions involving all three zeroes of P_0; these webs have the topology shown in the right side of Figure 5. For each of the 24 finite webs we worked out the corresponding charge γ following the rules of §3.9. This gives the 24 nonzero $\Omega(P_0, \gamma)$ listed in (5.13).

Acknowledgements

I am happy to thank Philip Boalch, David Dumas, Chris Fraser, Laura Fredrickson and Michael Wolf for very helpful discussions and explanations. I especially thank David Dumas for his assistance in understanding and using the code [1], which was of singular importance in confirming the details of the picture described here. This work was supported in part by NSF CAREER grant DMS-1151693 and a Simons Fellowship in Mathematics.

References

[1] D. Dumas and M. Wolf, "blaschke." https://github.com/daviddumas/blaschke.

[2] D. Dumas and M. Wolf, "Polynomial cubic differentials and convex polygons in the projective plane," *Geom. Funct. Anal.* **25** (2015), no. 6, 1734–1798, arXiv:1407.8149. MR3432157

[3] D. Gaiotto, G. W. Moore, and A. Neitzke, "Four-dimensional wall-crossing via three-dimensional field theory," *Commun. Math. Phys.* **299** (2010), 163–224, arXiv:0807.4723. MR2672801

[4] D. Gaiotto, G. W. Moore, and A. Neitzke, "Wall-crossing, Hitchin systems, and the WKB approximation," *Adv. Math.* **234** (2013), 239–403, arXiv:0907.3987. MR3003931

[21] A movie containing pictures of the networks $\mathcal{W}(P_0, \frac{n\pi}{300})_{n=0}^{99}$ is included with the arXiv version of this paper, as `hexagon.gif`.

[5] D. Gaiotto, G. W. Moore, and A. Neitzke, "Spectral networks," *Ann. Henri Poincaré* **14** (2013), 1643–1731, arXiv:1204.4824. MR3115984

[6] B. Dubrovin, "Geometry and integrability of topological-antitopological fusion," *Commun. Math. Phys.* **152** (1993), no. 3, 539–564, arXiv:hep-th/9206037. MR1213301

[7] S. Cecotti and C. Vafa, "On classification of $\mathcal{N} = 2$ supersymmetric theories," *Commun. Math. Phys.* **158** (1993), 569–644, arXiv:hep-th/9211097. MR1255428

[8] D. Dumas and A. Neitzke, "Opers and non-abelian Hodge: numerical studies," *Exp. Math.* (2021), 1–42. MR4713862

[9] C. Garza, "A construction of hyperkähler metrics through Riemann-Hilbert problems I," *Adv. Theor. Math. Phys.* **23** (2019), no. 6, 1533–1597, arXiv:1701.08188. MR4085681

[10] P. Boalch, "G-bundles, isomonodromy and quantum Weyl groups," *Int. Math. Res. Not.* **22** (2002) 1129–1166, arXiv:math/0108152. MR1904670

[11] C. Fraser, "Braid group symmetries of Grassmannian cluster algebras," *Sel. Math. New Ser.* **26** (2020), no. 2, Paper No. 17, 51, arXiv:1702.00385. MR4066538

[12] Z.-C. Han, L.-F. Tam, A. Treibergs, and T. Wan, "Harmonic maps from the complex plane into surfaces with nonpositive curvature," *Commun. Anal. Geom.* **3** (1995), no. 1-2, 85–114. MR1362649

[13] L. F. Alday and J. Maldacena, "Null polygonal Wilson loops and minimal surfaces in Anti-de-Sitter space," *J. High Energy Phys.* **11** (2009), 082, arXiv:0904.0663. MR2628869

[14] L. F. Alday, D. Gaiotto, and J. Maldacena, "Thermodynamic bubble ansatz," *J. High Energy Phys.* **09** (2011), 032, arXiv:0911.4708. MR2889878

[15] A. Fenyes, "Abelianization of SL(2,R) local systems," arXiv:1510.05757.

[16] M. Wolf, "High energy degeneration of harmonic maps between surfaces and rays in Teichmüller space," *Topology* **30** (1991), no. 4, 517–540. MR1133870

[17] Y. N. Minsky, "Harmonic maps, length, and energy in Teichmüller space," *J. Differ. Geom.* **35** (1992), no. 1, 151–217. MR1152229

[18] J. Loftin, "Flat metrics, cubic differentials and limits of projective holonomies," *Geom. Dedic.* **128** (2007), 97–106. MR2350148

[19] L. Katzarkov, A. Noll, P. Pandit, and C. Simpson, "Harmonic maps to buildings and singular perturbation theory," *Commun. Math. Phys.* **336** (2015), no. 2, 853–903, arXiv:1311.7101. MR3322389

[20] B. Collier and Q. Li, "Asymptotics of Higgs bundles in the Hitchin component," *Adv. Math.* **307** (2017), 488–558, arXiv:1405.1106. MR3590524

[21] R. Mazzeo, J. Swoboda, H. Weiss, and F. Witt, "Ends of the moduli space of Higgs bundles," *Duke Math. J.* **165** (2014), no. 12, 2227–2271, arXiv:1405.5765. MR3544281

[22] L. Katzarkov, A. Noll, P. Pandit, and C. Simpson, "Constructing buildings and harmonic maps," in: *Algebra, Geometry, and Physics in the 21st Century*, vol. 324 of *Progr. Math.*, pp. 203–260. Birkhäuser/Springer, Cham, 2017. arXiv:1503.00989. MR3727562

[23] T. Mochizuki, "Asymptotic behaviour of certain families of harmonic bundles on Riemann surfaces," *J. Topol.* **9** (2016), no. 4, 1021–1073, arXiv:1508.05997. MR3620459

[24] Z.-C. Han, "Remarks on the geometric behavior of harmonic maps between surfaces," in: *Elliptic and Parabolic Methods in Geometry* (Minneapolis, MN, 1994), pp. 57–66. A K Peters, Wellesley, MA, 1996. MR1417948

[25] D. Dumas, *Complex projective structures, grafting, and Teichmuller theory*. ProQuest LLC, Ann Arbor, MI, 2004. Thesis (Ph.D.) – Harvard University. MR2705981

[26] J. Acosta, "The asymptotics of representations for cyclic opers," arXiv:1609.06343.

[27] S. Cecotti, A. Neitzke, and C. Vafa, "R-twisting and 4d/2d correspondences," arXiv:1006.3435.

[28] F. Labourie, "Flat projective structures on surfaces and cubic holomorphic differentials," *Pure Appl. Math. Q.* **3** (2007), no. 4, 1057–1099. Special Issue: In honor of Grigory Margulis. Part 1, arXiv:math/0611250. MR2402597

[29] J. C. Loftin, "The compactification of the moduli space of convex $\mathbb{RP}^2$ surfaces. I," *J. Differ. Geom.* **68** (2004), no. 2, 223–276, arXiv:math/0311052. MR2144248

[30] N. J. Hitchin, "The self-duality equations on a Riemann surface," *Proc. Lond. Math. Soc. (3)* **55** (1987), no. 1, 59–126. MR0887284

[31] C. T. Simpson, "Higgs bundles and local systems," *Publ. Math. IHÉS* (1992), no. 75, 5–95. MR1179076

[32] K. Corlette, "Flat G-bundles with canonical metrics," *J. Differ. Geom.* **28** (1988), no. 3, 361–382. MR0965220

[33] S. K. Donaldson, "Twisted harmonic maps and the self-duality equations," *Proc. Lond. Math. Soc. (3)* **55** (1987), no. 1, 127–131. MR0887285

[34] C. Simpson, "Harmonic bundles on noncompact curves," *J. Am. Math. Soc.* **3** (1990), 713–770. MR1040197

[35] O. Biquard and P. Boalch, "Wild non-abelian Hodge theory on curves," *Compos. Math.* **140** (2004), no. 1, 179–204, arXiv:math/0111098. MR2004129

[36] T. Mochizuki, "Harmonic bundles and Toda lattices with opposite sign," *Commun. Math. Phys.* **328** (2014), no. 3, 1159–1198, arXiv:1301.1718. MR3201222

[37] L. Fredrickson and A. Neitzke, "Moduli of wild Higgs bundles on $\mathbb{C}P^1$ with $\mathbb{C}^\times$-actions," *Math. Proc. Camb. Philos. Soc.* **171** (2021), no. 3, 623–656. MR4324961

[38] C. Sabbah, "Harmonic metrics and connections with irregular singularities," *Ann. Inst. Fourier (Grenoble)* **49** (1999), no. 4, 1265–1291, arXiv:math/9905039. MR1703088

[39] N. J. Hitchin, "Lie groups and Teichmüller space," *Topology* **31** (1992), no. 3, 449–473. MR1174252

[40] H. L. Berk, W. M. Nevins, and K. V. Roberts, "New Stokes' line in WKB theory," *J. Math. Phys.* **23** (1982), no. 6, 988–1002. MR0659998

[41] T. Aoki, T. Kawai, S. Sasaki, A. Shudo, and Y. Takei, "Virtual turning points and bifurcation of Stokes curves for higher order ordinary differential equations," *J. Phys. A* **38** (2005), no. 15, 3317–3336, arXiv:math-ph/0409005. MR2132714

[42] A. Neitzke, "Cluster-like coordinates in supersymmetric field theory," *Proc. Natl. Acad. Sci.* **111** (2014), 9717–9724. MR3263304

[43] S. Fomin and P. Pylyavskyy, "Tensor diagrams and cluster algebras," *Adv. Math.* **300** (2016), 717–787. MR3534844

[44] D. Gaiotto, G. W. Moore, and A. Neitzke, "Framed BPS states," *Adv. Theor. Math. Phys.* **17** (2013), no. 2, 241–397, arXiv:1006.0146. MR3250763

[45] M. Alim, S. Cecotti, C. Cordova, S. Espahbodi, A. Rastogi, and C. Vafa, "$\mathcal{N} = 2$ quantum field theories and their BPS quivers," *Adv. Theor. Math. Phys.* **18** (2014), no. 1, 27–127, arXiv:1112.3984. MR3268234

[46] M. Alim, S. Cecotti, C. Cordova, S. Espahbodi, A. Rastogi, and C. Vafa, "BPS quivers and spectra of complete $N = 2$ quantum field theories," *Commun. Math. Phys.* **323** (2013) 1185–1227, arXiv:1109.4941. MR3106506

[47] A. Goncharov and L. Shen, "Donaldson-Thomas transformations of moduli spaces of G-local systems," *Adv. Math.* **327** (2018) 225–348. MR3761995

[48] P. Longhi, "Wall crossing invariants from spectral networks," *Ann. Henri Poincaré* **19** (2018), no. 3, 775–842, arXiv:1611.00150. MR3769247

[49] M. Kontsevich and Y. Soibelman, "Stability structures, motivic Donaldson-Thomas invariants and cluster transformations," arXiv:0811.2435.

[50] D. Joyce and Y. Song, "A theory of generalized Donaldson-Thomas invariants," arXiv:0810.5645. To appear in Memoirs of the A.M.S. MR2951762

[51] J. S. Scott, "Grassmannians and cluster algebras," *Proc. Lond. Math. Soc. (3)* **92** (2006), no. 2, 345–380, arXiv:math/0311148. MR2205721

[52] V. Fock and A. Goncharov, "Moduli spaces of local systems and higher Teichmüller theory," *Publ. Math. Inst. Hautes Études Sci.* (2006), no. 103, 1–211, arXiv:math/0311149. MR2233852

[53] A. Neitzke, "swn-plotter," http://gauss.math.yale.edu/~an592/mathematica/swn-plotter.nb.

Andrew Neitzke
Yale University
New Haven, CT
USA
E-mail address: andrew.neitzke@yale.edu

Received March 27, 2023; accepted October 28, 2023